ASSESSMENT OF WATER HAMMER EFFECTS ON BOILING WATER NUCLEAR REACTOR CORE DYNAMICS

by

Anis BOUSBIA-SALAH

Received on April 17, 2007; accepted on May 21, 2007

Complex phenomena, as water hammer transients, occurring in nuclear power plants are still not very well investigated by the current best estimate computational tools. Within this framework, a rapid positive reactivity addition into the core generated by a water hammer transient is considered. The numerical simulation of such phenomena was carried out using the coupled RELAP5/PARCS code. An overall data comparison shows good agreement between the calculated and measured core pressure wave trends. However, the predicted power response during the excursion phase did not correctly match the experimental tendency. Because of this, sensitivity studies have been carried out in order to identify the most influential parameters that govern the dynamics of the power excursion. After investigating the pressure wave amplitude and the void feedback responses, it was found that the disagreement between the calculated and measured data occurs mainly due to the RELAP5 low void condensation rate which seems to be questionable during rapid transients.

Key words: water hammer, coupled code simulation, kinetic thermal-hydraulic interaction

INTRODUCTION

In the last few years, computer code capabilities have been substantially improved, reaching a conciderable level of maturity, now capable of predicting nuclear power plant (NPP) behavior under a wide variety of transient and accidental conditions. However, phenomena such as water hammer, occuring regularly during a NPP lifetime, are still not very well investigated. In fact, rapid transients involving pressure waves could spread high dynamic loads over the plant's components and also generate rapid condensation in structures filled with steam or steam water mixtures. The latter effect could induce significant consequences on the kinetic equilibrium of a boiling water reactor (BWR) core. As outlined in several references in the literature, as [1] and [2], the modeling of such phenomenon remains a challenging topic for current computational tools. For this purpose, the BWR Peach Bottom Turbine Trip (PB-TT) test number 2 was investigated. The transient is initiated by a sudden closure of the turbine stop valve (TSV). This event leads to sonic pressure wave propagation through the steam lines and involves complex reflections from different solid and large fluid boundaries when it reaches the reactor vessel region. Due to the inherent feedback mechanisms, the core power exhibits a prompt excursion in response to the water hammer compressing effect, and immediately after that, a self-limiting shutdown course prior to the dropping of the control rod. In order to perform a best estimate (BE) simulation of such complex mechanisms, the coupled thermal-hydraulic system code RELAP5/Mod3 [3] and the 3-D neutronics code PARCS/2.3 [4] were used.

Afterwards, the calculated results were compared with the available experimental data. A good overall agreement between the calculated and experimental pressure wave amplitude and propagation was observed. However, the calculated power response exhibited less conformity to the measured one. Therefore, sensitivity studies, following the recommenda-

Scientific paper
UDC: 621.039.536:519.876.5
BIBLID: 1451-3994, *22* (2007), 1, pp. 18-33
DOI: 10.2298/NTRP0701018B

Author's address:
Department of Mechanical and Nuclear Engineering,
University of Pisa
2, Via Diotisalvi, 56126 Pisa, Italy

Author's e-mail:
b.salah@ing.unipi.it

tions of [5], have been carried out in order to identify the governing dynamic parameters of the TT transient.

WATER HAMMER PHENOMENON

Rapid transients involving pressure wave propagation across NPP structures occur regularly during their lifetime. At normal operation, water hammer occurs as a consequence of standard actions such as the start-up or shut-down of systems and components or the opening and closure of valves. It may also occur during the activation of emergency core cooling systems (ECCS) or auxiliary feed water systems. On the other hand, during out of the normal operations, such pipeline breakdowns are followed by rapid isolation valve closure and, in some instances, severe pressure waves involving complex reflections at different boundaries of fluid paths. Furthermore, this type of phenomena could lead to BWR instability. This could happen when TSV closures create oscillations corresponding to the core's coupled thermal-hydraulic-neutronic resonance frequency with associated amplifications. Generally, the water hammer transient has two aspects:

dynamic load "stresses" over the structures of the plant which could pose a serious problem for components previously damaged by various types of ageing, and

void condensation in structures filled with steam or steam water mixtures. The latter may have serious consequences on the kinetic equilibrium of a BWR core.

Once a pressure wave is produced in a pipeline, it propagates back and forth until it is completely dissipated. The effects associated with this phenomenon depend on the celerity of the pressure wave in relation to the rapidity of the rate of valve closure or opening. An illustration of the propagation and reflection of pressure waves in a simple configuration is shown in fig. 1. The system is composed of a pipeline connected to a big volume (RPV for example). The transient-state conditions are produced by instantaneously closing a downstream valve at time $t = 0$. The pressure wave is transmitted upstream at sonic velocity and reaches the supply reservoir in a time L/c. However, upon reaching the reservoir, it is reflected as a negative wave. In fact, pressure waves are true waves governed by the principles of wave mechanics. They can be reflected in two ways:

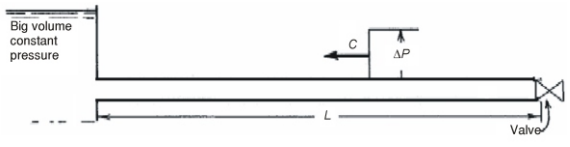

Figure 1. Simplified water hammer schema

either from a solid boundary, in which case velocity becomes zero while the pressure might vary, or

from a fluid boundary, in which case the pressure is constant, while the velocity might change.

Thus, when the pressure wave reaches the reservoir, it is reflected as an expansion wave with the same ΔP, but with opposite equal velocity. When it reaches the valve once more, it is reflected from the solid boundary, its velocity returns to zero and the pressure drops to $-P$ It then moves upstream to the reservoir where its negative pressure is eliminated by the reflection of an equal and opposite positive wave of forward velocity V. From the instant of valve closure, this latter wave reaches the valve after a time of $4L/c$. At this point, the pressure again drops to zero and its forward velocity equals V; consequently, the cycle will repeat itself and continue until it is eventually dampened out by the friction. The modeling of such phenomenon remains a challenging topic for existing computational tools, since it involves both core-plant interactions and strong feedback processes between kinetics and thermal-hydraulics. Both phenomena involve "time constants" in transient responses of pressure variations' propagation in specified flow paths and reactivity change characteristics, including time, magnitude, and spatial distribution aspects.

CALCULATION MODELS AND HYPOTHESES

The experiment was carried out by manually closing the TSV at an operating power level equal to 61.65% of its nominal value. Consequently, a pressure wave which propagates at sound velocity toward the reactor core is generated [6]. The pressure wave reaches the core zone following two different paths; through the steam separator filled with a mixture of water and steam and through the vessel downcomer filled with subcooled water. Therefore, the core void inventory is reduced under the water hammer pressurization effect, and due to the inherent feedback mechanisms, induces a rapid exponential rise in reactor power. To relax the water hammer loads, the steam by-pass valve (BPV) opens automatically after 0.06 s and core power is scramed when it exceeds 95% of its nominal value. The pressure wave (or water hammer phenomenon) constitutes a thermal-hydraulic problem, not well characterized by the existing system codes. The propagation of the pressure wave from the turbine inlet to the core could be better represented by 3-D simulation, especially in the RPV zone, since complex reflections are involved.

To perform a numerical simulation of the TT transient, the coupled code RELAP5 Mod3.3/PARCSV2.4 code was used. In fact, the RELAP5 modules simulate, mainly, the pressure wave propagation, as well as the evo-

lution of the core thermal-hydraulic parameters, having as an input the 3-D power response derived by the PARCS code routines. The codes are run separately through a parallel virtual machine process. During the TT transient, complex kinetic and thermal-hydraulic feedback mechanisms are involved. Consequently, it is essential to simulate adequately the propagation and the amplitude of the pressure wave through the steam line and different structures of the reactor vessel. The RELAP5 code is a widely used and qualified BE thermal-hydraulic system code. Nevertheless, the code was rarely used for investigation of the water hammer phenomenon in single and two-phase flow through complex structures [7, 8]. Furthermore, according to [2], using the code for water and steam hammer analyses is a controversial topic. Basically, the donor-cell differential schemes used by RELAP5 to resolve the momentum conservation equation have shown that for nodalization schemes used by most thermal-hydraulic analysts in RELAP5-type problems, an acoustic wave is rapidly attenuated. Thus, very close attention must be paid to plant nodalization, *i. e.* cell size and time step. In particular, when the pressure wave is expected to have a very rapid rate of increase, cell nodalization should have small length dimensions. To fulfill these requirements, a peach bottom plant nodalization, as shown in fig. 2, was performed and validated against a series of steady-state and transient sensitivity analyses [9]. The nodding scheme includes various vessel components, such as a steam separator, steam dome, downcomer, and coolant recirculation loops, including two jet pumps. The attention is focused on steam line nodalization, since the leading phenomenon is the pressure wave propagation. As shown in fig. 2, which exhibits the sketch of the adopted PB plant nodalization flow diagram, the four real steam lines are lumped into two components and a constant node size of 1.0 m was chosen over a total length of 140 m for each steam line. The correspondence between the plant component and their relative node number is shown in tab. 1.

CALCULATION RESULTS

The BWR PB-TT is a pressure-driven scenario, therefore it is important to catch the right pressure wave amplitude and peak timing. Notwithstanding the reliability of the 3-D kinetics code, the results will be off if the pressure wave is not accurately predicted. The predicted pressure wave propagation upstream and downstream the steam lines in comparison with experimental data is shown in figs. 3 and 4, respectively. The calculated pressure wave propagation agrees qualitatively well with the measurements; the

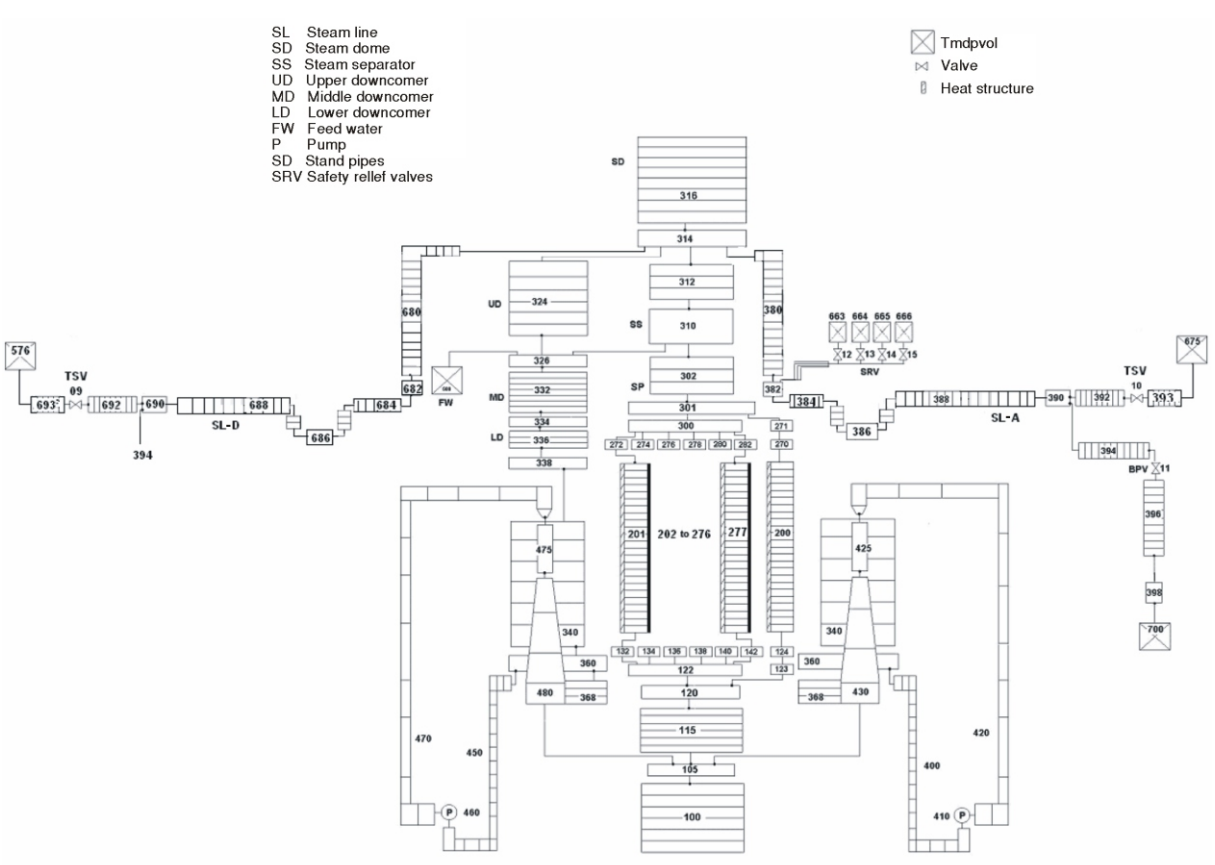

Figure 2. Nodalization scheme of the Peach Bottom

Table 1. Main nodalization items for the RELAP5 input deck

Plant component	Node type	Node number
Lower plenum	Pipe Branch	100, 105 115
Core inlet	Branch	120, 122
Core	Pipe	201-233
Core by-pass	Pipe	123, 124, 200, 270, 271
Upper plenum	Branch	300, 301
Stand-pipes	Pipe	302
Separators	Branch	310
Steam dome	Pipe branch	312, 314 316
Upper downcomer	Annulus	324
Middle downcomer	Branch annulus	326 332
Lower downcomer	Branch annulus	334, 338, 360 336, 340, 368
Steam line A (SL-A) Steam line D (SL-D)	Pipe branch Pipe branch	380, 384, 388 382, 386 680, 684, 688 682, 686
Steam by-pass chest	Pipe	394
Steam by-pass line	Pipe	396
Steam by-pass orifice	Branch	398
Recirculation suction	Pipe	400-450
Recirculation discharge	Pipe	420-470
Pump	Pump	410-460
Jet pump throat discharge	Jetmixer Pipe	425-475 430-480
Turbine stop valve (TSV)	Valve	10
By-pass valve (BPV)	Valve	11
Safety relief valve	Valve	12
Relief valves	Valve	13, 14, 15
Feedwater	Tmdpvol	500
Turbine	Tmdpvol	675
Condenser	Tmdpvol	700

overall trend is well predicted, especially for the pressure data in SL-A. The differences between the measured and calculated amplitudes could be due to measurement and boundary and/or initial conditions (BIC) uncertainties and, more particularly, to the assumed linear TSV closure mode. This mode is adopted since the real dynamic behavior of valves is generally unknown. The effects of such modeling are considered in more detail in the sensitivity studies' section.

When the pressure wave reaches the reactor vessel, it experiences several reflections, mainly with the vessel walls. The resultant wave propagates through two different paths to reach the core zone; the steam separator filled with the mixture of water and steam and the lower plenum filled with subcooled water. The calculated pressure wave in the RPV dome is shown in comparison to the one measured in fig. 5. The calculated trends exibit a good agreement with both the amplitude and the rate of increase of the measured pressure wave.

Wave propagation through the downcomer and core inlet is performed with practically no attenuations since the path is filled with water. However, when the wave crosses the steam separator, it experiences a strong deceleration (see fig. 6) without significant attenuation, as can be seen in fig. 7. However, the real behavior of pressure wave propagation through the separator will not be well simulated since a basic component is used in the current RELAP5 nodalization. Nevertheless, a qualitatively good pressure wave in the upper zone of the core is predicted. Furthermore, the calculated and measured pressure waves exhibit the same fundamental oscillatory mode. This parameter could be evaluated by a simple formula given in the case of straight pipeline pressure wave propagation toward a big reservoir [10]:

$$\frac{1}{\tau} \quad \frac{4L}{c} \quad ^{1} \quad \frac{4\ 140}{480} \quad ^{1} \quad 0.86\,\text{Hz} \qquad (1)$$

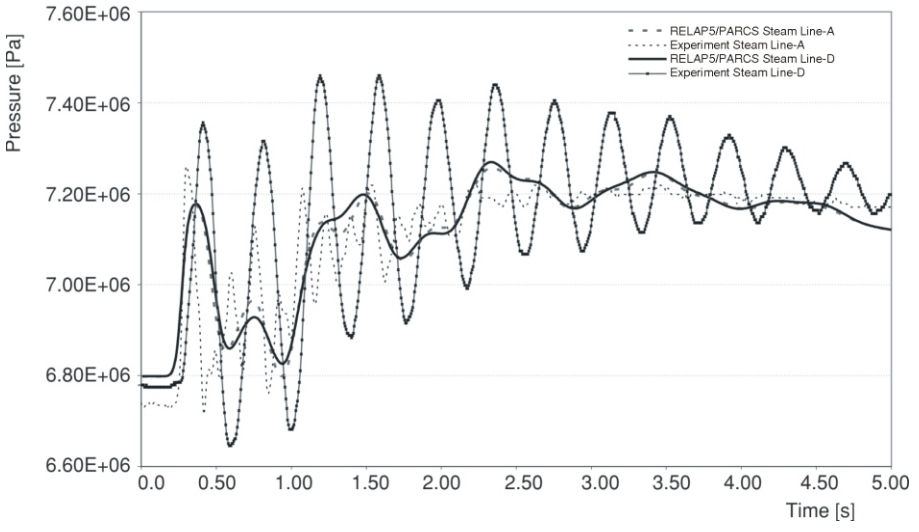

Figure 3. Calculated and experimental data of the pressure wave upstream the turbine zone

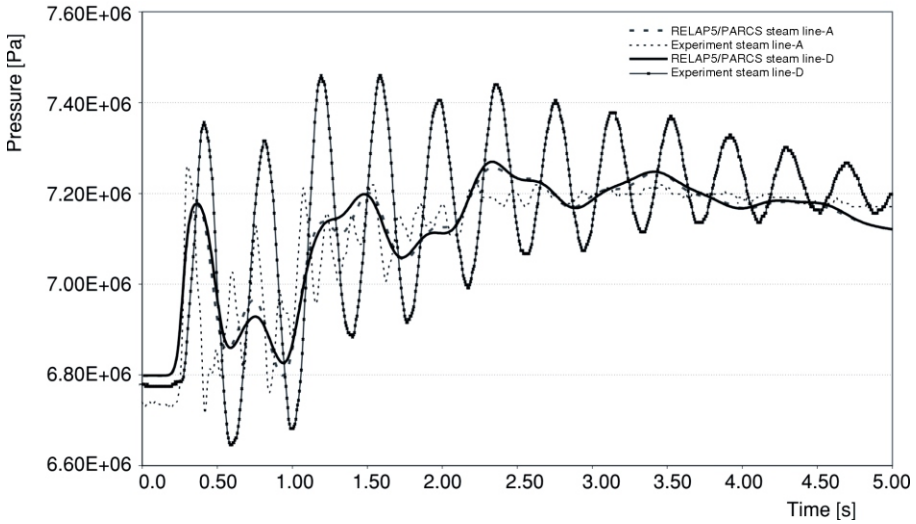

Figure 4. Calculated and experimental data of the pressure wave evolution in the steam line

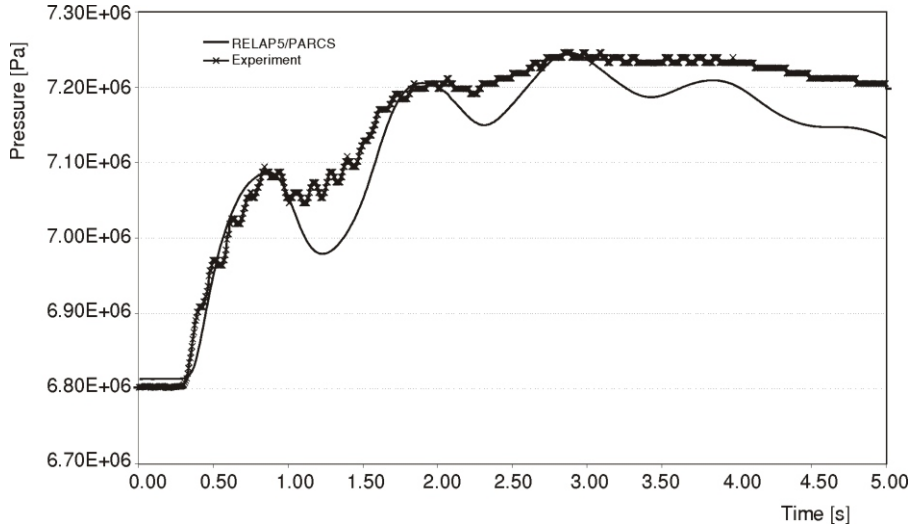

Figure 5. Calculated and experimental data of the pressure wave evolution in steam dome

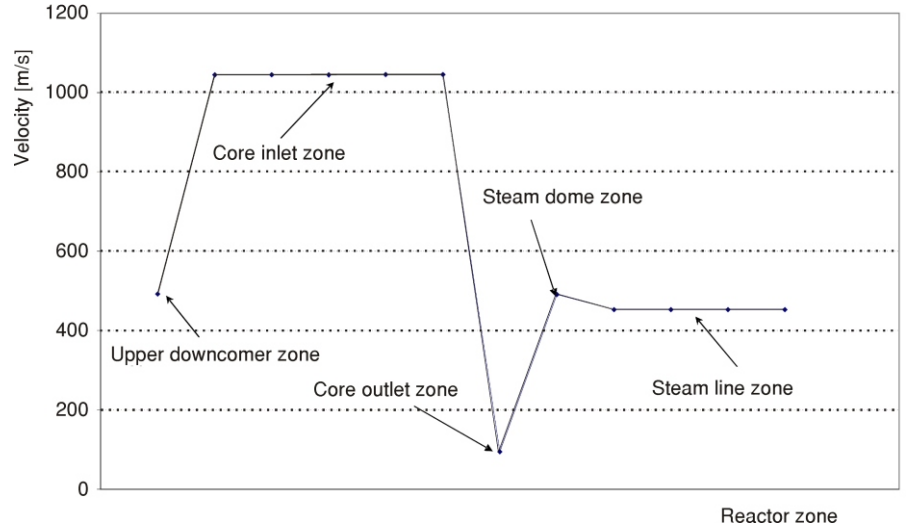

Figure 6. Sound velocity in different reactor regions

where: τ, L, and c are the wave period, the steam line length, and the mean sound velocity in the steam line, respectively.

The so-called "steam line period" (eq. 1) corresponds, more or less, to the calculated and measured wave frequency. The oscillating trend observed in the

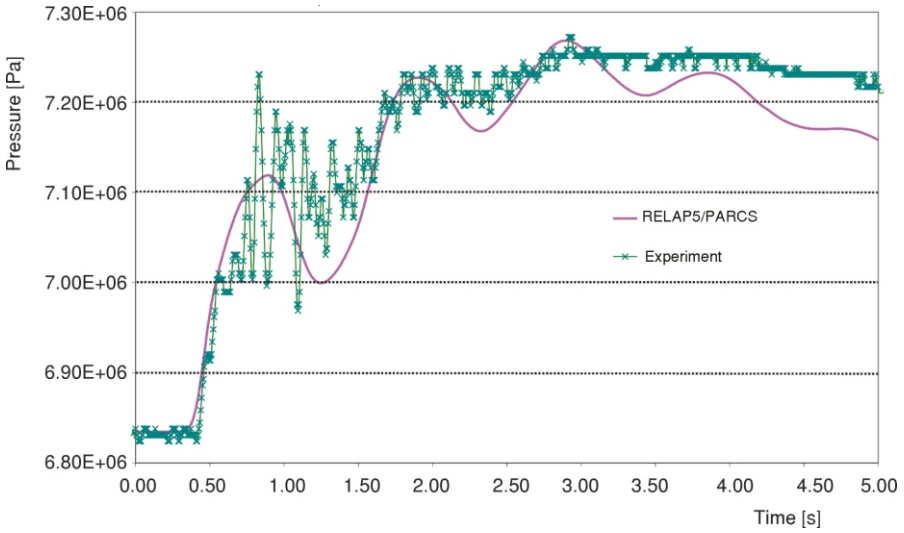

Figure 7. Core outlet pressure evolution

measured pressure is a consequence of the dynamic effect of the control rod insertion during the shutdown phase [11]. The current model is not able to predict this effect. The calculated pressure response occurs approximately a 0.1 s earlier than the experimental one. The reasons for this anticipated response are likely due to the differences between the real and calculated sonic velocities (the degree of different coolant mixtures in various locations of the pressure wave paths). For the core pressure wave, the calculated trend agrees well with the measured data, even though some small differences, mostly arising from uncertainties connected with code predictions [5], such as the adopted valves dynamic characteristics or the nodalization model for the steam line, can be observed.

Owing to the inherent feedback mechanisms, the void collapse, induced by the pressure wave action, results in a positive reactivity insertion. The amount of inserted reactivity makes the total system reactivity evolve near to the prompt critical zone. Thereby, the power response exhibits a prompt exponential rise with a decreasing period and prompt self-limiting behavior prior to shutdown. The calculated power course, in comparison to the measured one, is sketched in fig. 7. The discrepancies observed for the power response are more pronounced, even though qualitatively similar error trends to those of the pressure wave are expected. The main difference between the two power profiles appears during the excursion phase. The coupled code calculations predict slower power exponential rise at the beginning of the excursion phase and, consequently, a lower power peak is predicted.

SENSITIVITY CALCULATIONS

In order to identify and assess the discrepancies between the measurements and code calculations for both the pressure wave and power response, a series of sensitivity cases are considered, as outlined in tab. 2. According to [5], discrepancies between code predictions and the measurements could be attributed to

Table 2. List of the considered sensitive cases

Parameter	Case number	Description
Steam line nodalization	Case-1 Case-2 Case-3	Steam line with mesh node size = 0.5 m Steam line with mesh node size = 2.0 m Steam line with mesh node size = 8.0 m
BIC related to turbine stop valve closure	Case-4 Case-5	TSV closure time changed by +20% TSV closure time changed by 20%
BIC related to by-pass valve opening	Case-6 Case-7	BPV opening time changed by +20% BPV opening time changed by 20%
Control systems delays	Case-8 Case-9	BPV opens as 0.07 s (instead of 0.06 s) BPV opens as 0.05 s (instead of 0.06 s)
Uncertain NPP data	Case-10 Case-11 Case-12 Case-13	Steam dome volume 20% Steam dome volume 20% BPV flow area 10% BPV flow area +10%
Void model	Case-14 Case-15 Case-16	CATHARE subcooled model Umbrella of Void condensation correlation

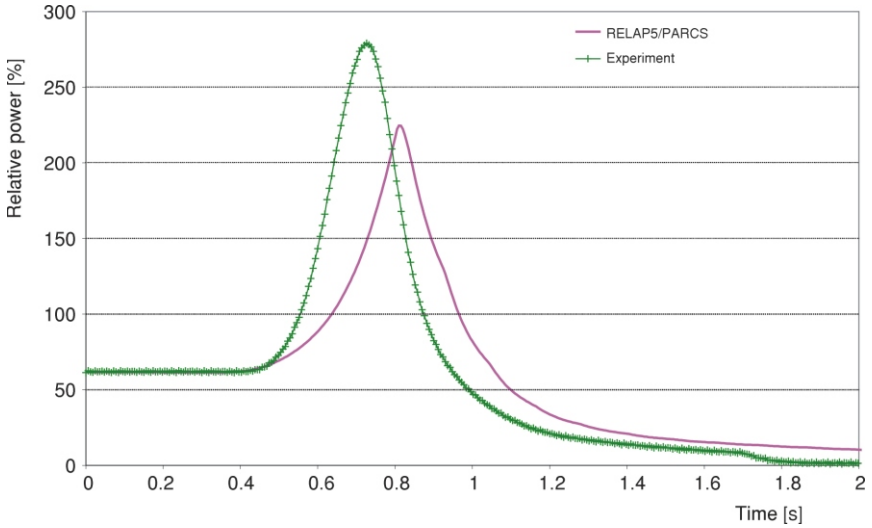

Figure 8. Reactor power response during the transient

model deficiencies (inadequacy of correlations embedded in the code), approximation in the numeric solutions, nodalization inadequacies or imperfect knowledge of detailed NPP design data, control system delays, as well as boundary and initial conditions.

Pressure response

The dependence of pressure wave damping on steam line nodalization and on uncertainties associated with the BIC are considered in cases 1 to 10. The effect of steam line nodalization is considered in cases 1 to 4, while cases 5 to 10 deal with uncertainties related to closure and opening times of the TSV and BPV.

Nodalization effect

The intial cases investigated here deal with the effect of node size on pressure wave damping. As can be seen in figs. 9 and 10, as well as in tab. 3, it seems that pressure wave and power trends are insensitive to node sizes smaller than 2.0 m. On the other hand, a coarse node of a size of 8.0 m causes significant damping of the pressure wave amplitude and a somewhat earlier occurrence of the core's pressure initial response. Consequently, as shown in fig. 10, the power response is predicted to occur slightly earlier and a lower power peak, due to a smaller amount of inserted positive reactivity, is obtained. Therefore, it seems that the steam line nodalization effect is not significant enough (if reasonable node sizes are chosen) to significantly dampen the resulting pressure wave amplitude and, consequently, power response.

Boundary and initial conditions

Most of the BIC related to any experimental tests involve a degree of measurement uncertainties. This is particularly true of valve components of unknown characteristics, especially the dynamic ones, their true effects often having to be evaluated from sensitivity

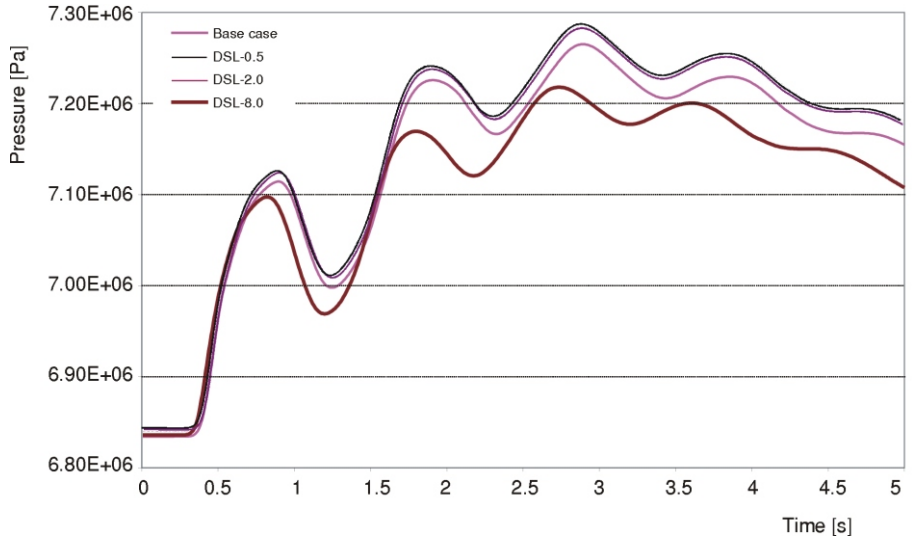

Figure 9. Core pressure wave evolution for various steam line node numbers

analyses. As outlined in [12], there is a direct dependence between the valve closure/opening dynamics and the maximum amplitude of the developed pressure. For this purpose, two extreme linear modes of TSV closure time were considered. The base case time closure was first reduced and then increased by 20%. The effects of such changes are presented in fig. 11 for the pressure wave and in fig. 12 for the power response. As can be seen in tab. 3, the time of the initial pressure response does not exhibit any significant changes. The same goes for the amplitudes of the pressure wave and the power peak changes; their variation does not exceed 2%.

The effect of the BPV opening time interval is assessed in cases 7 and 8, while cases 9 and 10 deal with the initial time of the BPV opening. As can be seen in figs.13 and 14, the effect of the BPV opening time on the transient course is significant. The amplitude of the pressure wave, as well as of the power peak, vary between 6% and 10%. However, the time of the power peak occurrence does not change significantly in all the aforementioned BIC cases.

Control system response

The control system effect on thermal-hydraulic and kinetic system responses is significant since it governs the activation of several safety systems which have a direct influence on the behaviour of the system as a whole. In the following study, the influence of delayed and earlier BPV opening on the TT course is investigated. Results of coupled code calculatins are outlined in tab. 3 and sketched in figs. 15 and 16. As can be seen, the effects of the BPV opening control system did not affect significantly the calculated TT transient course either in the case of the pressure wave or that of power trends.

Uncertain NPP data

Probably the most uncertain NPP data which could influence the TT course are the BPV-flow area (BPV-FA) and steam dome volume (SDV). For this purpose, sensitivity calculations were performed by varying the SDV by ±20% and the BPV flow area by

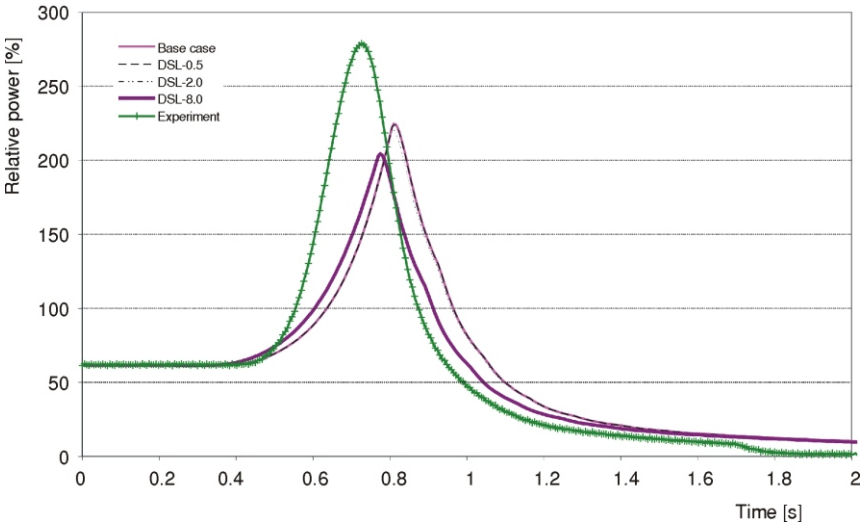

Figure 10. Core power evolution for different steam line nodalizations

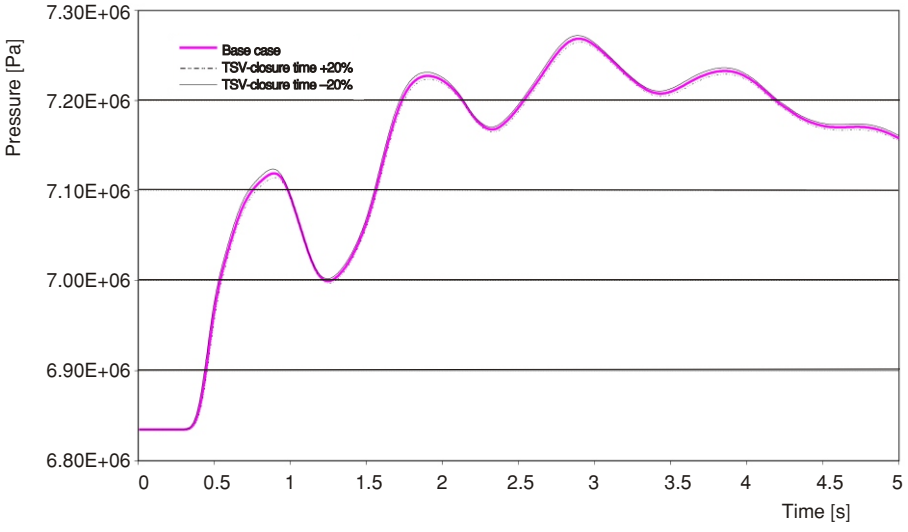

Figure 11. Core pressure wave evolution for different TSV time closure

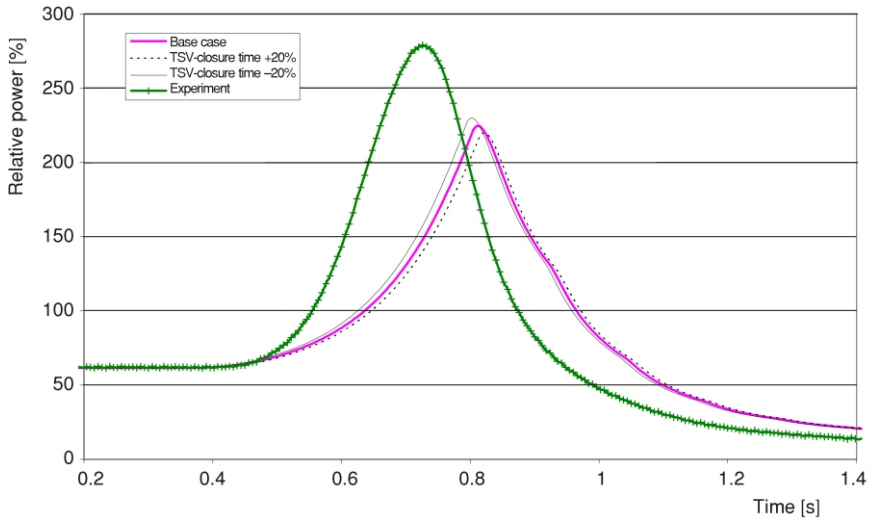

Figure 12. Core power evolution for different TSV time closure

±10%. The effects of such variations on pressure and power responses are sketched in figs.17 to 20. The impact of a SDV change is more emphasized than the BPV-FA effect, since a higher pressure wave amplitude was obtained from a reduced SDV (–20%). In this case, the pressure wave is less diffused in the vessel dome and, consequently, lower exponential excursion periods are obtained. However, the obtained power response does not correspond to the experimental one and remains far from the experimental trend.

Feedback response

The feedback response is closely dependent upon the thermal-hydraulic closure relationships implemented into the code. In RELAP5/3.3 there are few

Table 3. Considered cases for the sensitivity analyses

Case	Amplitude of pressure wave [MPa]		Initial pressure response [s]		Relative peak power [%]		Peak power time occurrence [s]	
Experiment or reference	0.303	Error [%]	0.426	Error [%]	279.1	Error [%]	0.726	Error [%]
Base case	0.284	6.3	0.387	9.2	224.7	19.5	0.810	11.6
Case-1	0.284	6.3	0.387	9.2	224.0	19.7	0.810	11.6
Case-2	0.284	6.3	0.387	9.2	221.0	20.8	0.809	11.4
Case-3	0.261	13.9	0.360	15.5	204.5	26.7	0.775	6.80
Case-4	0.280	7.6	0.396	7.0	220.0	21.2	0.820	12.9
Case-5	0.289	4.6	0.380	10.8	229.9	17.6	0.800	10.2
Case-6	0.310	2.3	0.387	9.2	239.7	14.1	0.810	11.6
Case-7	0.250	17.5	0.390	8.5	201.5	27.8	0.815	12.3
Case-8	0.290	4.3	0.388	8.9	226.0	19.0	0.810	11.6
Case-9	0.279	7.9	0.390	8.5	226.0	19.0	0.810	11.6
Case-10	0.286	5.6	0.368	13.6	240.6	13.8	0.800	10.2
Case-11	0.266	12.2	0.375	12.0	223.4	20.0	0.850	17.1
Case-12	0.300	1.0	0.387	9.1	232.0	16.9	0.810	11.6
Case-13	0.269	11.2	0.388	8.9	212.6	23.8	0.810	11.6
Case-14	0.290	4.3	0.388	9.2	273.0	2.40	0.720	0.8
Case-15	0.284	6.3	0.390	9.2	232.1	16.9	0.800	10.2
Case-16	0.266	12.2	0.418	1.9	274.7	1.60	0.730	0.5

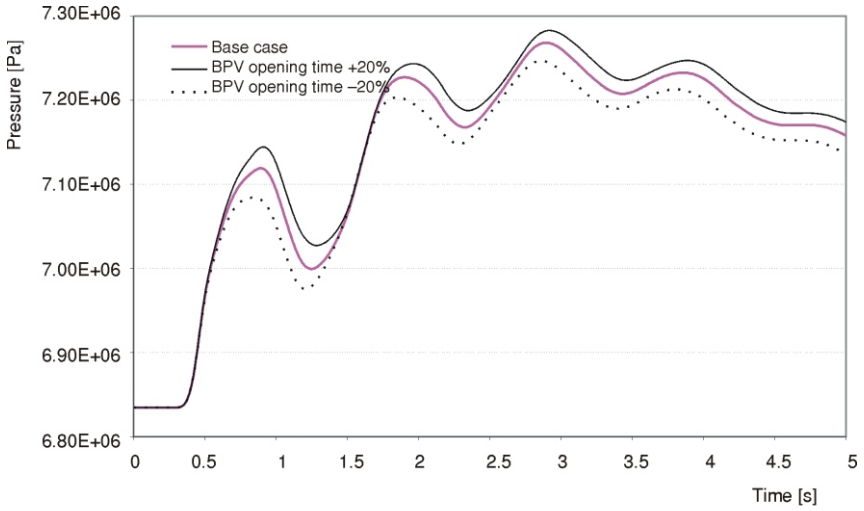

Figure 13. Core pressure wave evolution for different BPV opening conditions

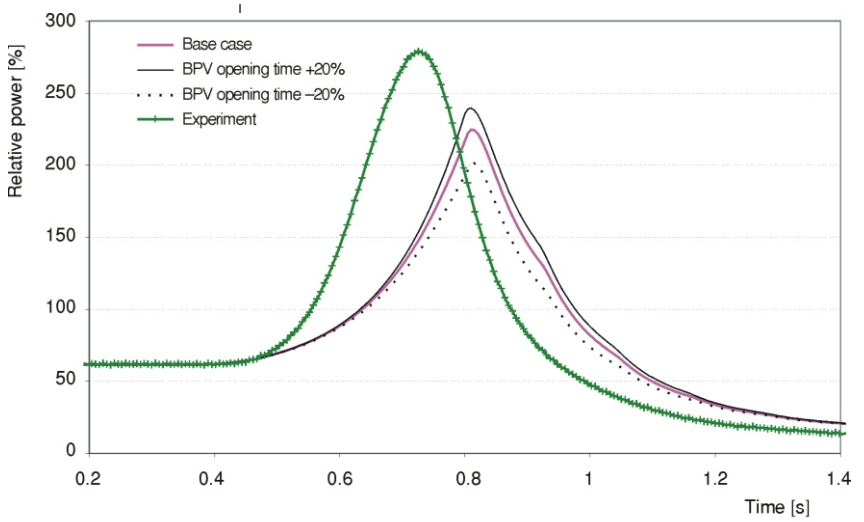

Figure 14. Core power evolution for different BPV opening conditions

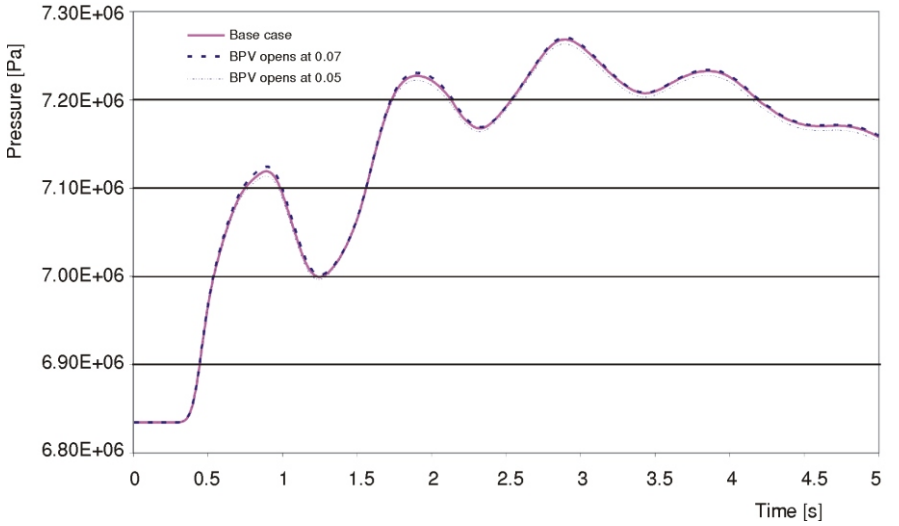

Figure 15. Core pressure wave evolution for different BPV opening times

possibilities to investigate different models for a given phenomenon. However, for the subcooled model there is a possibility to use the CATHARE [13] model for this boiling regime, by removing the Umbrella restriction or by implementing a new closure relationship for the condensation rate.

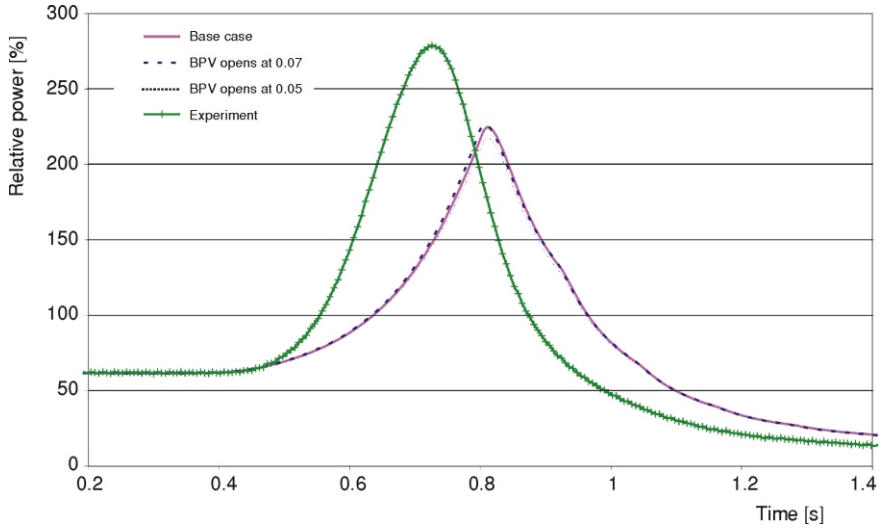

Figure 16. Core power evolution for different BPV opening times

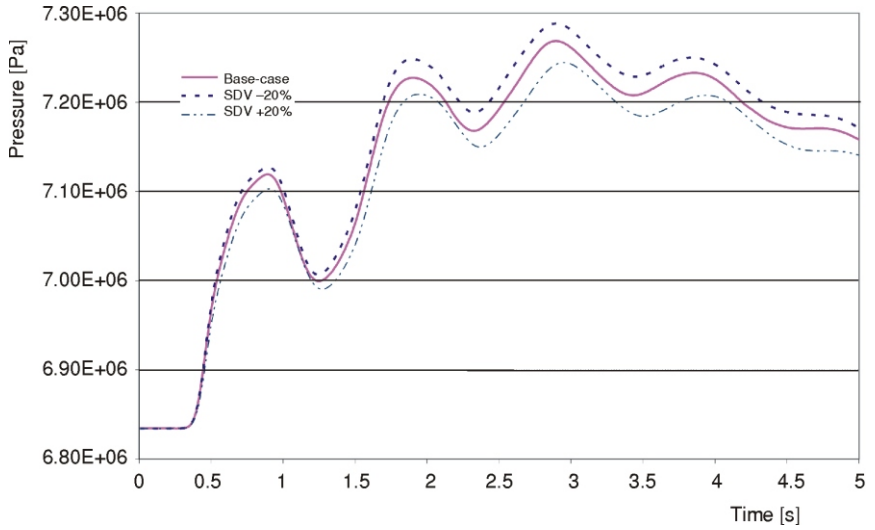

Figure 17. Core pressure wave evolution for different values of the steam dome volume

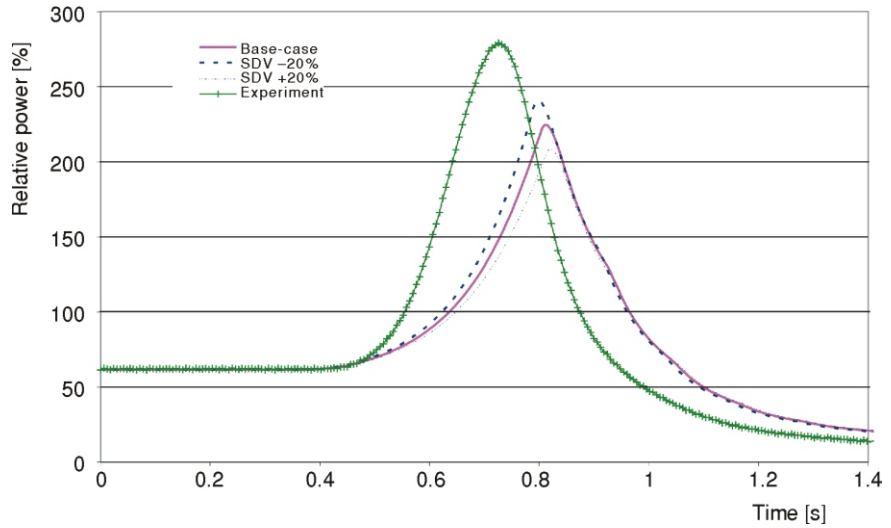

Figure 18. Core power for different values of the steam dome volume

CATHARE subcooled model

The results of such calculations are sketched in figs. 21 and 22 for the core pressure and power, respectively. As can be seen, the pressure wave profile is similar to the base case, but the rate of the amplitude rise is slightly more pronounced (see tab. 3). The power response is much more improved in compari-

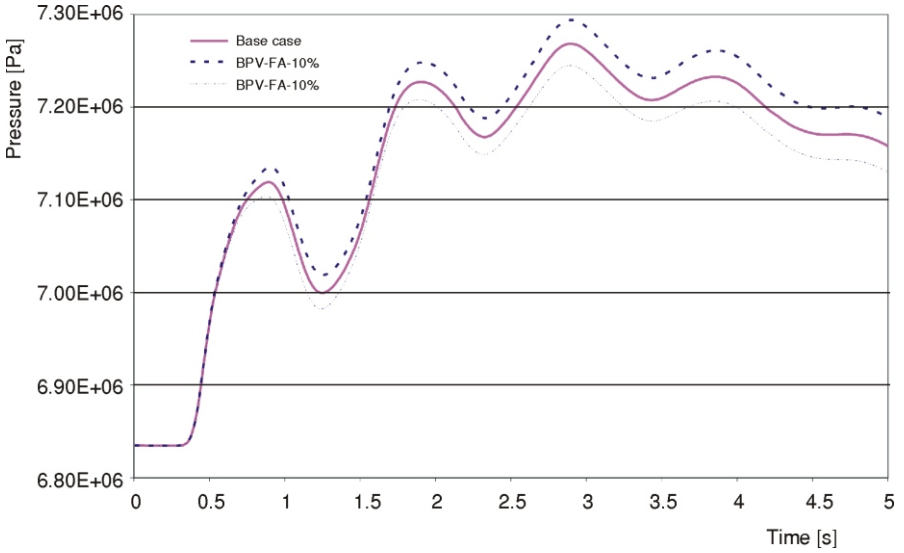

Figure 19. Core pressure wave evolution for different BPV flow area

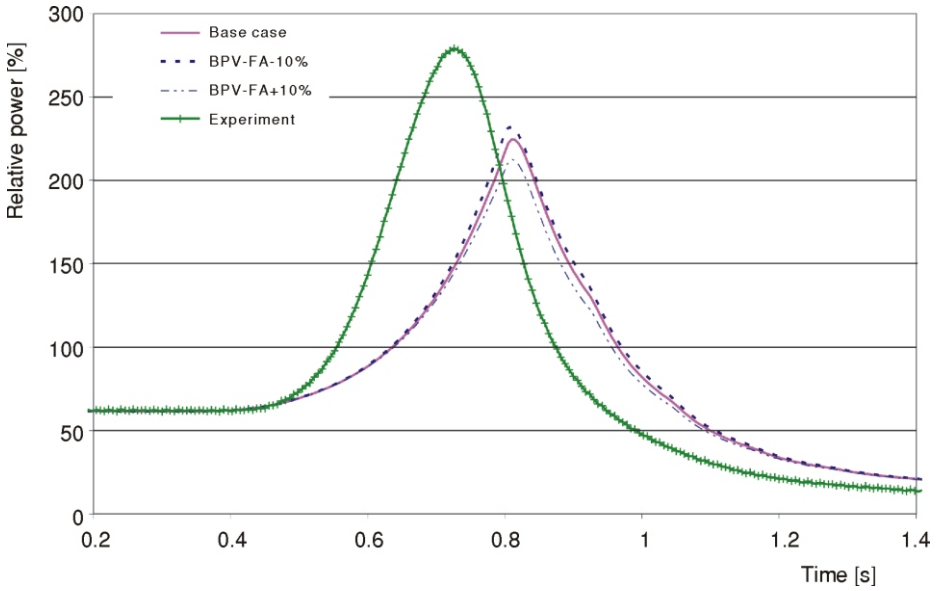

Figure 20. Core power evolution for different BPV flow area

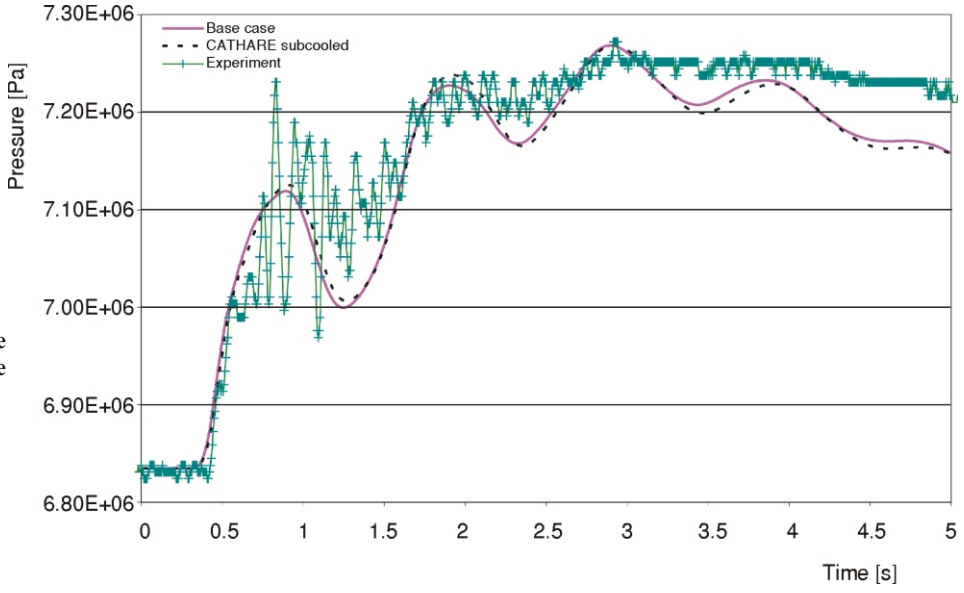

Figure 21. Core pressure wave evolution using the CATHARE subcooled boiling model

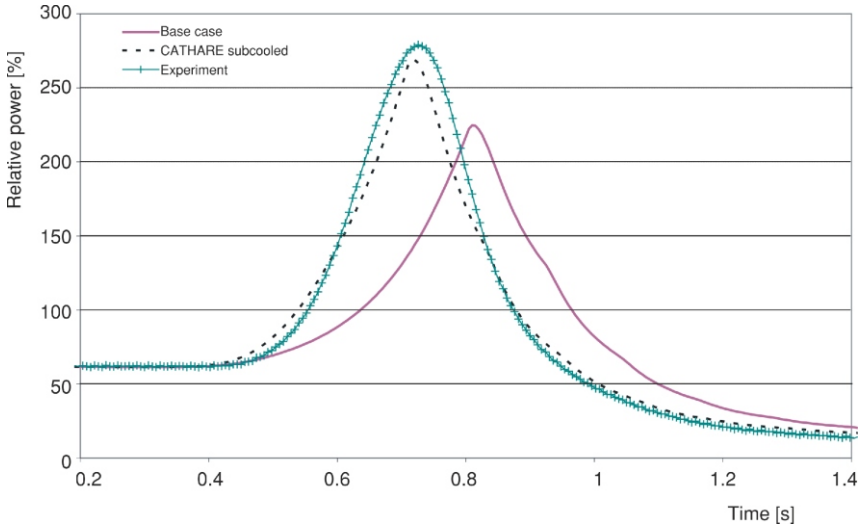

Figure 22. Core power evolution using the CATHARE changes to the subcooled boiling model

son with the base case. Power excursion is much faster and closer to the experimental trend.

The Umbrella restriction

The void condensation model may be investigated by removing the Umbrella restriction (see eq. 4) or by investigating the condensation rate. The results of the switching off of the Umbrella restriction of the power course are sketched in fig. 23. Slightly faster power excursion is obtained, indicating that a higher void condensation is predicted. However, the overall power trend remains far from the measured one.

Void condensation correlation

The condensation rate is a function of the local subcooling as well as of the interfacial area concentration and the interfacial heat transfer coefficient. In RELAP5/3, it is evaluated through the Unal-Lahey mechanistic correlation [14] given by the following formula:

$$\Gamma_c \quad \frac{H_{\text{if}}(T^{\text{sat}} \quad T_{\text{f}})}{h_{\text{g}}^{\text{sat}} \quad h_{\text{f}}^{\text{sat}}} \tag{2}$$

where

$$H_{\text{if}} \quad \frac{F_3 F_5 (h_{\text{g}}^{\text{sat}} \quad h_{\text{f}}^{\text{sat}}) \rho_{\text{g}} \rho_{\text{f}} \alpha}{\rho_{\text{f}} \quad \rho_{\text{g}}} \tag{3}$$

Factor F_3 is equal to 1 in the case of liquid subcooling less than 1.0 K. Factor F_5 has been introduced as a smoothing factor between the Lahey and Unal models. The condensation model implemented in the RELAP5 code is governed by the so called Umbrella restriction so as to force the volumetric interfacial heat transfer coefficient H_{if} to small values as the void fraction (α) approaches either 0 or one [14]

$$H_{\text{if}} \quad \min \quad H_{\text{if}}, 17.539 \max[4.724, 472.4\alpha(1 \quad \alpha)]$$

$$\max\ 0, \min\ 1, \frac{\alpha \quad 1.0.10 \quad 10}{0.1 \quad 1.0.10 \quad 10} \tag{4}$$

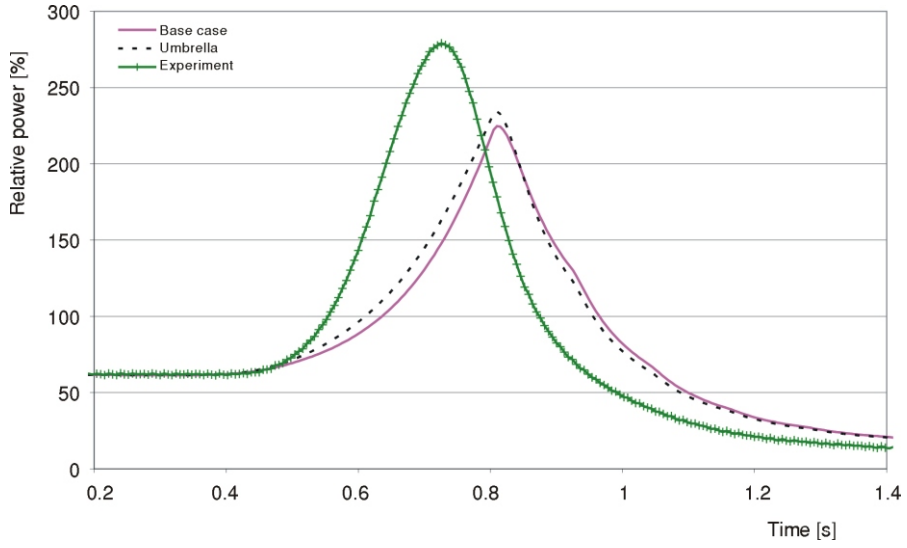

Figure 23. Core power evolution without considering the Umbrella restriction

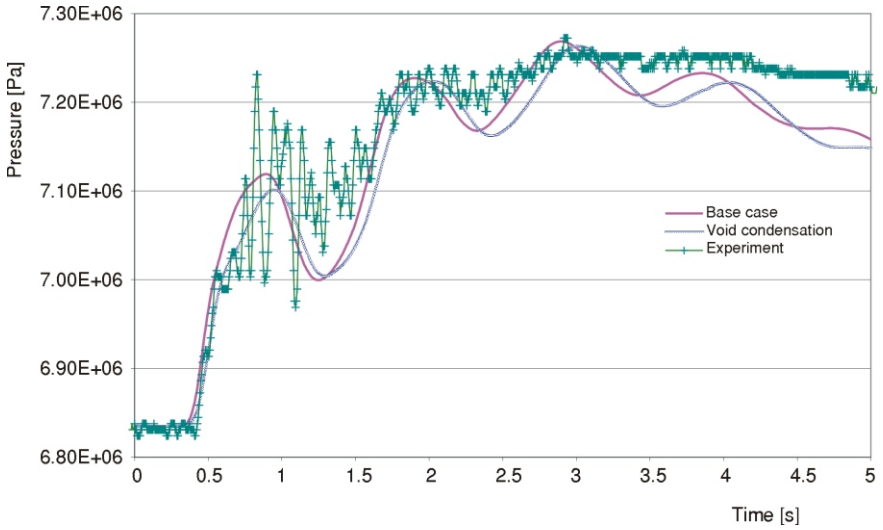

Figure 24. Core pressure wave evolution considering different condensation model

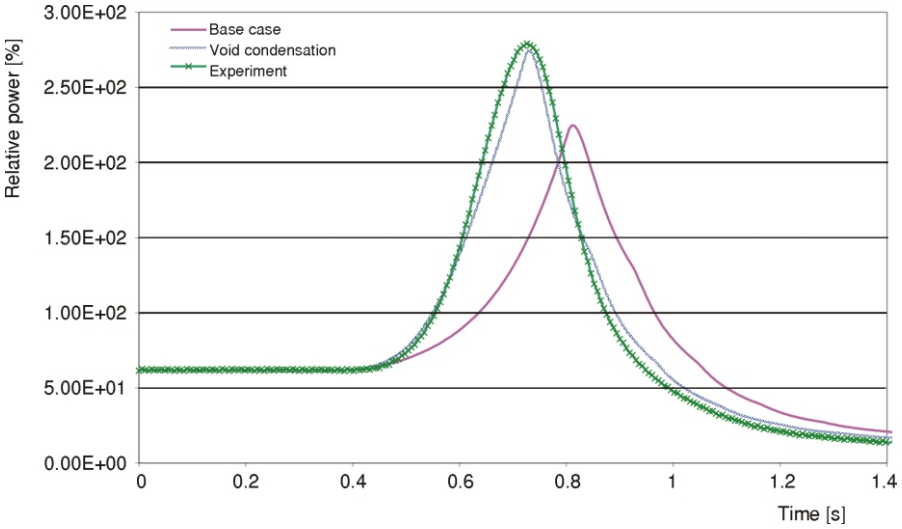

Figure 25. Core power evolution considering different condensation models

On the other hand, according to [15], the RELAP5 model calculates too low condensation rates, at least at low-pressure conditions. This also seems to be the case for the current study involving rapid dynamic effects, even though the operating pressures are high.

In order to check the latter possibility, the RELAP5 code was compiled using the alternative void condensation closure equation proposed by [15]. The effect of such a modification is shown in figs. 24 and 25 which present the evolutions of the pressure wave and core power, respectively. In this case, the time of the initial pressure response is closer to the experimental one. Other key parameters are also well predicted, since only minor errors have been detected in this case, as outlined in tab. 3. The power excursion phase coincides well with the experimental trend. Significant improvements over the base case calculations are obtained as well.

According to the obtained results, it is clear that, even though a correct trend of the core pressure is predicted by code calculations, the prompt feedback mechanisms remain weak and insensitive to the pressure wave amplitude variations; the calculated overall trend of the core power, especially the prompt response, remains relatively removed from the measured one. Therefore, the predominant effect governing the power course seems to be related to the void dynamics in the subcooled boiling zone.

CONCLUSION

Recent advancements in numerical methods and computer power have enhanced the possibilities of gathering a global vision of NPP system behavior during complex transient scenarios. Within this framework, an aspect related to the simulation of the BWR turbine trip water hammer induced positive reactivity has been considered. The coupled code technique by means of the RELAP5-PARCS code was used, since complex and strong feedback interactions between the

core kinetics and thermal-hydraulics are involved. Preliminary calculations predicted a correct trend of pressure wave propagation from the steam lines to the core zone. However, slower power excursion with respect to the experimental response was observed. Therefore, a series of sensitivity analyses were performed in order to identify the origin of the observed discrepancies. It was established that:

- a correct trend of the pressure wave propagation through different components of the reactor is predicted if a normal or common nodalization of the steam lines is performed,
- more efficinet BE thermal-hydraulic simulation will be obtained if 3-D RPV modeling is performed. This will, for instance, allow adequate simulation of the pressure wave reflections and inlet core mass flow rates for each individual channel,
- the effect of valves' dynamics on pressure wave amplitude and kinetic behaviour is significant, and
- it was found that the RELAP5 closure relationships estimate a low void condensation rate, and consequently, incorrect prompt feedback mechanisms were predicted. The use of alternative void models gives closer results to the experimental trends.

The current study also emphasizes the importance of uncertainty evaluations of best estimate code predictions. Nevertheless, further assessment studies and investigations should be performed to improve the reliability of code predictions.

NOMENCLATURE

c – sound velocity
L – pipe length
h – enthalpy
H_{if} – interfacial heat transfer coefficient
P – pressure
V – velocity
α – void fraction
τ – oscillation period
ρ – density

Superscripts

f – liquid phase
g vapor phase

Subscript

sat – saturation conditions

REFERENCES

[1] Giot, M., Prasser, H. M., Dudlik, M., Ezsol, A. G., Habip, M., Lemonnier, H., Tiselj, L., Castrillo, F., Van Hove, W., Perezagua, R., Potapov, S., Two-Phase Flow Water Hammer Transients and Induced Loads on Materials and Structures of Nuclear Power Plants (WAHALoads), *Proceedings,* FISA 2001 EU Research in Reactor Safety, Luxemburg, November 12-14, 2001

[2] Tiselj, I., Horvat, A., Accuracy of the Operator Splitting Technique for Two-Phase Flow with Stiff Source Terms, *Proceedings*, ASME FEDSM'02, 2002 ASME Fluids Engineering Division Summer Meeting, Montreal, Canada, 2002, FEDSM 2002-31349

[3] Ransom, V. H., Wagner, R. J., Trapp, J. A., Johnsen, G. W., Miller, C. S., Kiser, D. M., Riemke, R. A., RELAP5/MOD3 Code Manual: User Guide and Input Requirements, NUREG/CR-4312 EGG-2396, 1990

[4] Joo, H. G., Barber, D., Jiang, G., Downar, T. J., PARCS, A Multi-Dimensional Two Group Reactor Kinetics Code Based on the Nonlinear Analytic Nodal Method, PU/NE-98-26, 1998, NRC-V1.00

[5] D'Auria, F., Chojnacki, E., Glaeser, H., Lage, C., Wickett, T., Overview of Uncertainty Issues and Methodologies, OECD/CSNI Seminar on Best Estimate Methods in Thermal Hydraulic Safety Analysis. NEA/CSNI/R(99) 10, 1999

[6] Carmichael, L. A., Niemi, R. O., Transient and Stability Tests at Peach Bottom Atomic Power Station Unit 2 at End of Cycle 2, EPRI NP-564, 1978

[7] Tietsch, W., Applicability of RELAP for Special T&H Problems. Simulation of Pressure Waves in Branched Fluid Systems, Fall CAMP Meeting 2002, Alexandria, VA, USA, 2002

[8] ***, RELAP5 Code Development Team, RELAP5/MOD3 Code Manual, Volume IV: Models and Correlations, NUREG/CR-5535, Scientech, Inc., Idaho Falls, ID, USA, 1999

[9] Bousbia-Salah, A., D'Auria, F., Analysis of the Peach Bottom 2 BWR Turbine Trip Experiment by RELAP5/Mod3.2., *Nuclear Technology & Radiation Protection, 17* (2002), 1-2, pp. 44-49

[10] Roberson, J. A., Cassidy, J. J., Chaudhry, M. H., Hydraulic Engineering, John Wiley & Sons Editions, New York, USA, 1997

[11] Hornyik, K., Naser, J. A., RETRAN Analysis of the Turbine Trip Tests at Peach Bottom Atomic Power Sation Unit 2 at the End of Cycle 2, EPRI-NP-1076-SR, 1979

[12] Morris, H. M., Wiggert, J. M., Applied Hydraulics in Engineering, John Wiley & Sons Editions, New York, USA, 1992

[13] Bestion, D., Dossier Descriptif CATHARE MI.4-Description Générale des lois Physiques du Module de Base,. SETh: LEML-EM: 89-190, 1990

[14] Fletcher, C. D., Schultz, R. R., RELAP5/MOD3 Code Manual, vol. IV, User's Guidelines,. Idaho National Engineering Laboratory, Idaho Falls, ID, USA, NUREG/CR-5536, INEL-95/0174, 1995

[15] Končar, B., Mavko, B., Modeling of Low-Pressure Subcooled Flow Boiling Using the RELAP5 Code, *Nuclear Engineering and Design, 220* (2003), pp. 255-273

Анис БУСБИА-САЛАХ

ПРОЦЕНА ЕФЕКАТА ХИДРАУЛИЧНОГ УДАРА НА ДИНАМИКУ ЈЕЗГРА НУКЛЕАРНОГ РЕАКТОРА СА КЉУЧАЛОМ ВОДОМ

Сложена дешавања као што су појаве транзијената хидрауличног удара у нуклеарним електранама још увек нису довољно добро истражене савременим рачунарским средствима за најбољу прогнозу. У овим оквирима, разматрано је нагло додавање позитивне реактивности језгру настало транзијентом хидрауличног удара. Нумеричка симулација те појаве извршена је коришћењем спрегнутог RELAP5/PARCS програма. Целовито поређење података показује добро слагање између рачунатих и мерених промена таласа притиска у језгру. Међутим, предвиђени одговор снаге током фазе екскурзије није правилно одразио експериментално понашање. Ради овога, спроведене су студије осетљивости с циљем да се препознају најутицајнији параметри који управљају динамиком екскурзије снаге. После испитивања амплитуде таласа притиска и повратних одговора шупљина, утврђена је да се несагласност рачунатих и мерених података појављује углавном услед ниске брзине кондензације шупљина у програму RELAP5, која се чини недовољно познатом током брзих транзијената.

Кључне речи: хидраулични удар, симулација спрегнутим кодом, кинетичка термо-хидраулична интеракција